BioNanoScience (2019) 9:883–892
https://doi.org/10.1007/s12668-019-00666-4

Influence of Cross-linking Agents on Drug Delivery Behavior of Magnetic Nanohydrogels Made of Polyvinyl Alcohol and Chitosan

Hamidreza Shagholani[1] · Sayed Mehdi Ghoreishi[2] · Reza Rahmatolahzadeh[3]

Published online: 8 August 2019

Abstract
With the purpose of examining cross-linking agents, we used glutaraldehyde and ammonium persulfate to synthesize nanohydrogels based on poly(vinyl alcohol), chitosan, and magnetite nanoparticles. Fe_3O_4 nanoparticles were produced by coprecipitation in alkaline solution under sonication followed by coating with chitosan. Then, poly(vinyl alcohol) was combined with chitosan in the presence of glutaraldehyde and ammonium persulfate as cross-linking agents. The Fe_3O_4 nanoparticles had nanoscale size that was confirmed by XRD, SEM, and TEM. VSM measurements showed that all samples were superparamagnetic. Physicochemical properties of nanohydrogels were measured by DLS and zeta potential. The unspecific adsorption and interaction of nanohydrogels with bovine serum albumin and immunoglobulin G were investigated systematically by UV-Vis spectroscopy method. The release profile of nanohydrogels showed that nanohydrogels cross-linked with glutaraldehyde represent more sensitivity to pH. These nanohydrogels had more and faster release in acidic release medium.

Keywords Fe_3O_4 nanoparticles · Chitosan · Poly(vinyl alcohol) · Drug delivery · Cross-linking agent

1 Introduction

Drug delivery devices and systems have been developed along with advances in material design and engineering. Therefore, new materials with more complexity and functionality have been applied into this field [1]. Drug delivery systems based on nanoparticle platforms is considered a suitable approach for overcoming the limitations of traditional drug formulations. In traditional approaches, drug molecules could diffuse and distribute freely throughout the body, resulting in undesirable toxic side effects. Using nanoparticles as nanocarries can be a suitable method in several distinct disease conditions. They have long circulation lifetimes and could be accumulated at target sites. Therefore, safety and tolerability will be improved [2–4].

✉ Hamidreza Shagholani
Shagholani@khayam.ut.ac.ir

[1] Institute of Nanoscience and Nanotechnology, University of Kashan, Kashan, I.R, Iran

[2] Department of Analytical Chemistry, Faculty of Chemistry, University of Kashan, Kashan, I.R, Iran

[3] Tehran Firefighting Center of Applied Science and Technology, Tehran, I.R, Iran

When nanoparticles are loaded with therapeutic agents, they can perform as efficient drug delivery systems. By using appropriate nanocarries, non-specific cell interactions could be minimized and have more control on drug release. Moreover, by using an imaging agent, delivery tracking could be achieved. Nanoparticles as nanodrug carriers need careful physicochemical and targeting design. For these purpose, further considerations paid to drug loading, transport, and release are required. The rate and mechanism of drug release must be adjusted for optimal therapeutic efficacy. For instance, the concentration and duration of release of therapeutic agent after uptake by cell could be predetermined. Furthermore, the release of drug could be modulated or triggered at an optimal site and time [5].

Drug release generally refers to transportation of encapsulated drug molecules to the surface of matrix and then into surrounding environment [6]. Local and rate release of therapeutic agents depend on matrix properties, drug properties, and environmental factors. Many factors have been mentioned that they can affect on the degradation and drug release of polymers, such as flow rate, residual solvents, buffer concentration, porosity, temperature, size of the matrix, shape, drug solubility, crystallinity, weight-average molecular weight, composition, and enzymes [7, 8].

Craciun et al. reported that the release of drug strongly depends on its encapsulation into the pores of system. They

showed that the diffusion process of drugs into or out of hydrogels was controlled by the microporous channel morphology of system. Fine encapsulation of the drug led to a prolonged release by slowing down its dissolution and diffusion [9].

The hydrogels could act as biomedical carriers to reach the target tissue and then release drugs to cure diseases [10]. Many papers reported hydrogels based on chitosan, either for tissue repair or as drug delivery systems for the treatment of various diseases and especially tumors. Chitosan has fascinating biopharmaceutical properties such as pH sensitivity, biocompatibility, biodegradability, mucoadhesivity, low toxicity, and low immunogenicity. It can be cross-linked with different types of cross-linking agents, to provide nanoparticles with efficient network for entrapment of drug molecules [11, 12].

On the other hand, poly(vinyl alcohol) (PVA) has been studied in several advanced biomedical and biological applications because of its biocompatibility, non-toxicity, desirable physical properties, and high swelling. Interests on hydrogels based on PVA which blended with polysaccharides or some other synthetic polymers are due to the abundance of these polymers, easy modification, and biocompatibility [13, 14]. In this work, magnetic nanohydrogels of PVA and chitosan are synthesized with different cross-linking agents. By using paramagnetic nanoparticles, it could be possible to guide and propel them to a desired direction [15]. For example, it has been shown that controlled transport and guidance of cells could be achieved via an external magnetic field [16].

To investigate the influence of cross-linking agents, these nanohydrogel systems were synthesized with glutaraldehyde (GA) and ammonium persulfate (APS) as cross-linking agents. Nanohydrogels were loaded with ascorbic acid as a model of drug, and their release kinetics have been investigated in vitro.

2 Experimental

2.1 Materials

$FeCl_2.4H_2O$, $FeCl_3.6H_2O$, PVA with molecular weight of 72000 g/mol, GA, APS, aqueous ammonia (NH_4OH, 25 wt%), acetic acid, and bovine serum albumin (BSA) were all purchased from Merck & Co. Chitosan with medium molecular weight and deacetylation degree of ≥ 75% was obtained from Sigma-Aldrich. Immunoglobulin G (IgG) protein solution (50 mg/mL) was provided from Kashan University of Medical Sciences.

2.2 Synthesis of Fe_3O_4 Nanoparticles

Fe_3O_4 nanoparticles were synthesized according to our previous work [17]. $FeCl_3.6H_2O$ and $FeCl_2.4H_2O$ (2:1 molar ratio) were dissolved in deionized water, and the vessel was placed into ultrasonic bath. Ammonia was added to solution during sonication under inert atmosphere. The sonication was continued for 15 min, and then, the obtained black magnetic nanoparticles were separated with a strong magnet. The separated nanoparticles were washed with deionized water and ethanol to remove the impurities and unreacted material. The nanoparticles were dried in 50 °C for 24 h before further use.

2.3 Coating of Fe_3O_4 Nanoparticles with Chitosan (Ch–Fe_3O_4)

Fe_3O_4 nanoparticles were dispersed in deionized water by sonication for 10 min. Separately, chitosan was dissolved in water-acetic acid solution by stirring and a light heating. Dispersed nanoparticles were added to chitosan solution, and the mixture was stirred at 700 rpm, for 12 h, at room temperature. During this time, chitosan molecules were placed onto the surface of nanoparticles. Then, the obtained nanoparticles were separated by centrifugation at 12000 rpm. Ch–Fe_3O_4 nanoparticles were washed with deionized water and dried at room temperature.

2.4 Synthesis of Nanohydrogels

0.25 g of PVA was dissolved in 60 mL of deionized water at 60 °C. Separately, 0.1 g of Ch–Fe3O4 NPs homogeneously dispersed in 15 mL of deionized water by sonication. These solutions were mixed together and stirred to obtain a homogeneous dispersion.

Reaction in the Presence of GA (PVA-GA-Fe_3O_4 Nanohydrogels) After 15 min, 0.15 mL of GA and 1 mL of HCl (1 M) were added to the mixture, respectively. The mixture was stirred at a speed of 800 rpm for 15 min and then separated by a strong magnet. The product was washed with deionized water twice and dried at room temperature.

Reaction in the Presence of APS (PVA-APS-Fe_3O_4 Nanohydrogels) Ten milliliters of ammonium persulfate solution (0.2 g) was gradually added to dispersion. The mixture was stirred for 4 h at a speed of 800 rpm and at 60 °C. After that, the obtained nanohydrogels were magnetically separated and washed with deionized water. Then, nanohydrogel was dried at room temperature.

2.5 Iron Content

The amount of solid content and polymer coating in nanohydrogels was quantified by an atomic absorption spectrophotometer (Perkin-Elmer 2380, air/C_2H_2). For this purpose, each nanomaterial was precisely weighted. Nanomaterials were digested in 5 mL of HCl. These solutions

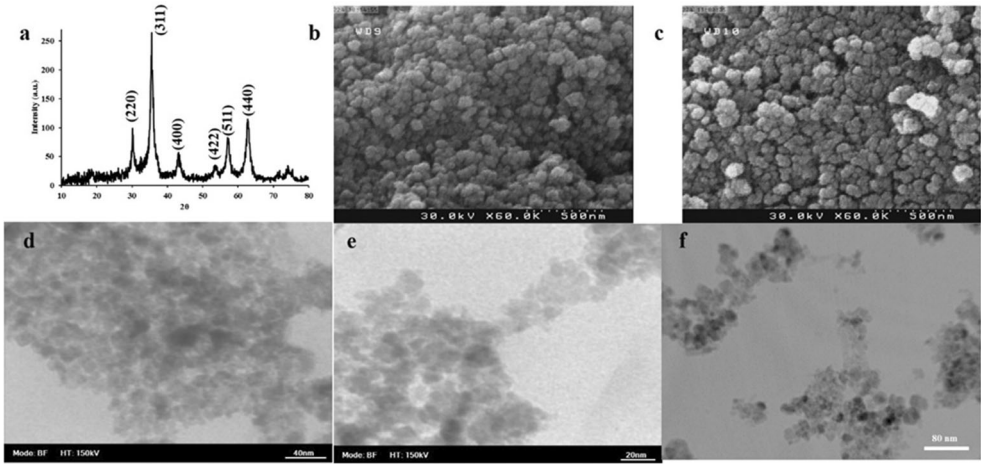

Fig. 1 **a** XRD pattern of Fe_3O_4. **b** SEM image of Fe_3O_4. **c** SEM image of Ch–Fe_3O_4. **d**, **e** TEM images of Fe_3O_4. **f** TEM image of Ch–Fe_3O_4nanoparticles

were maintained overnight. Then, the solutions were diluted to 50 mL by adding deionized water. The concentration of iron in each solution was measured by using a calibration curve. Then, the amount of coating in nanomaterials was calculated from the amount of iron in them.

2.6 Protein Adsorption Studies

The obtained nanomaterials were dispersed sonicated in 10 mL of BSA and IgG solutions (1 mg/mL). The dispersions were remained for 24 h at 37 °C and then separated by centrifugation. Non-adsorbed proteins in the supernatant were measured by using a UV-Vis spectrophotometer (Purkinje General Instrument, Beijing, China), and the absorbance was recorded between 255 and 295 nm.

2.7 Drug Loading and Release Experiments

Ascorbic acid was used as a model of drug to examine drug loading and in vitro release behavior of nanohydrogels. To

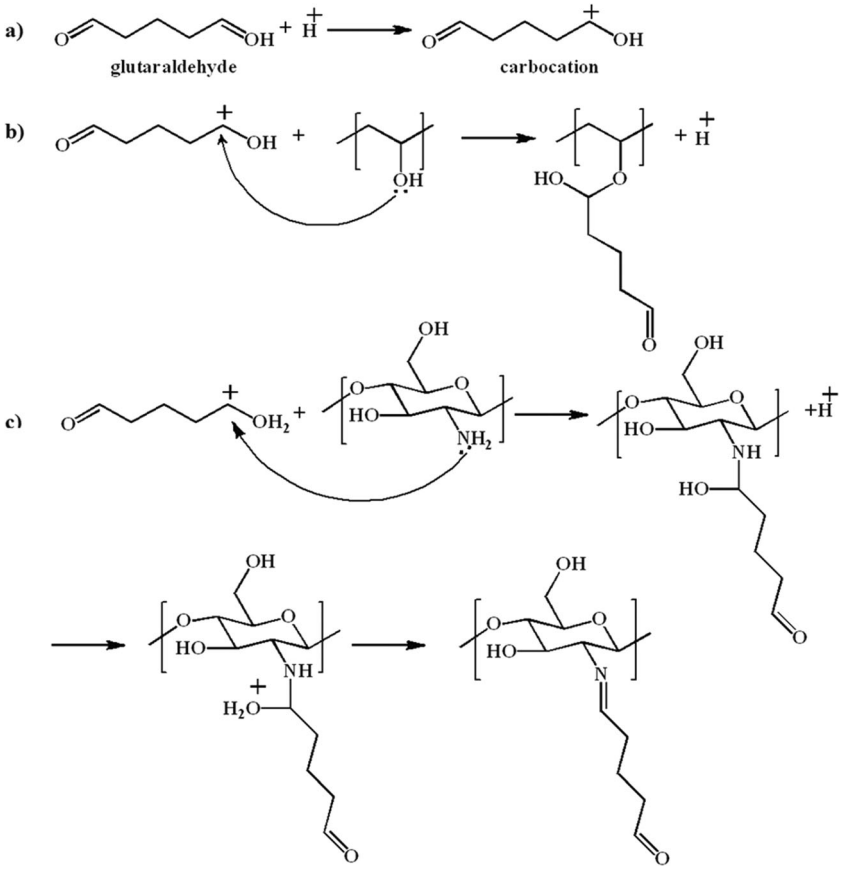

Scheme 1 Cross-linking process of nanohydrogels treated with GA

Scheme 2 Cross-linking process of nanohydrogels treated with PVA

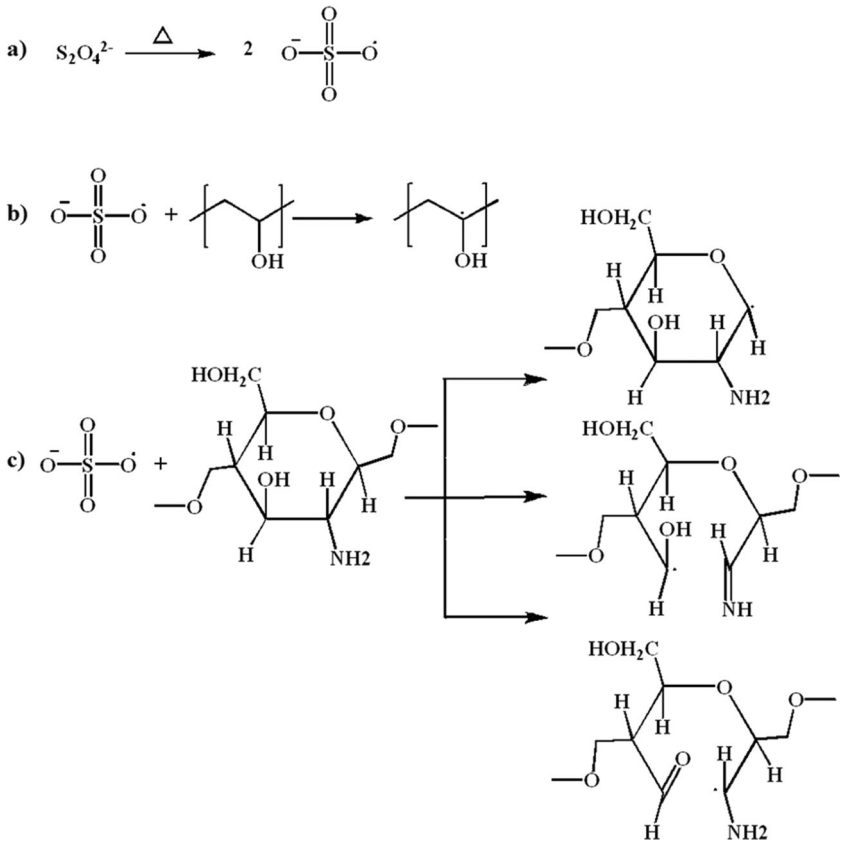

load ascorbic acid, a dispersion of ascorbic acid and nanohydrogels (50% w/w) was prepared by sonication. The mixture was kept for 24 h at room temperature, and then, nanohydrogels were separated from solution by a magnet. The amount of reminded drug in solution was measured by a UV-Vis spectrophotometer to estimate drug loading in nanohydrogels. The drug loading contents and drug entrapment efficiency of nanohydrogels were calculated as follows:

$$\text{drug loading contents } (\%) = \frac{\text{weight of drug in NPs}}{\text{weight of prepared NPs}} \times 100$$

$$\text{drug entrapment efficiency } (\%) = \frac{\text{weight of durg in NPs}}{\text{weight of drug injected}} \times 100$$

The in vitro release was performed in 100 mL of phosphate-buffered saline (PBS) solution with pH = 7.4 and 5.8, at 37 °C to investigate the effects of cross-linking agents. The drug release profiles of nanohydrogels were estimated by the dialysis method. A precise amount of drug-loaded nanohydrogels and 3 mL of PBS was placed in a dialysis membrane bag with molecular weight cutoff of 14 kDa. Then, the dialysis bag was immersed into 100 mL of PBS solution. At specific time points, 3 mL of samples were collected for analysis and replaced with fresh buffer. The released ascorbic acid concentration was detected by UV-Vis absorbance spectroscopy at 254 nm.

3 Result and Discussion

Fe_3O_4 nanoparticles were synthesized using coprecipitation method and the sonication of ferric and ferrous salts in basic environment. Then, these nanoparticles were modified and functionalized with chitosan. Powder X-ray diffraction (XRD) was applied to study crystallinity Fe_3O_4 nanoparticles. XRD was performed by a Philips X-ray diffractometer (X'Pert Pro) using Cu Kα radiation (λ = 1.54060 Å). The diffraction data was obtained at 2θ values from 10 to 80° at room temperature. XRD pattern of Fe_3O_4 nanoparticles is shown in Fig. 1a. From the pattern, it can be suggested that they are in highly crystalline state. Six characteristic peaks corresponding to reflection planes are shown by their indices (2 2 0), (3 1 1), (4 0 0), (4 2 2), (5 1 1), and (4 4 0). These peaks are related to the spinel structure of magnetite phase (Fe_3O_4, reference JCPDS no. 82-1533). Moreover, the broad peaks of the pattern indicated that Fe_3O_4 nanoparticles were in nanoscale sizes. The mean crystallite size has been obtained using Scherrer's formula which is 24.6 nm [18].

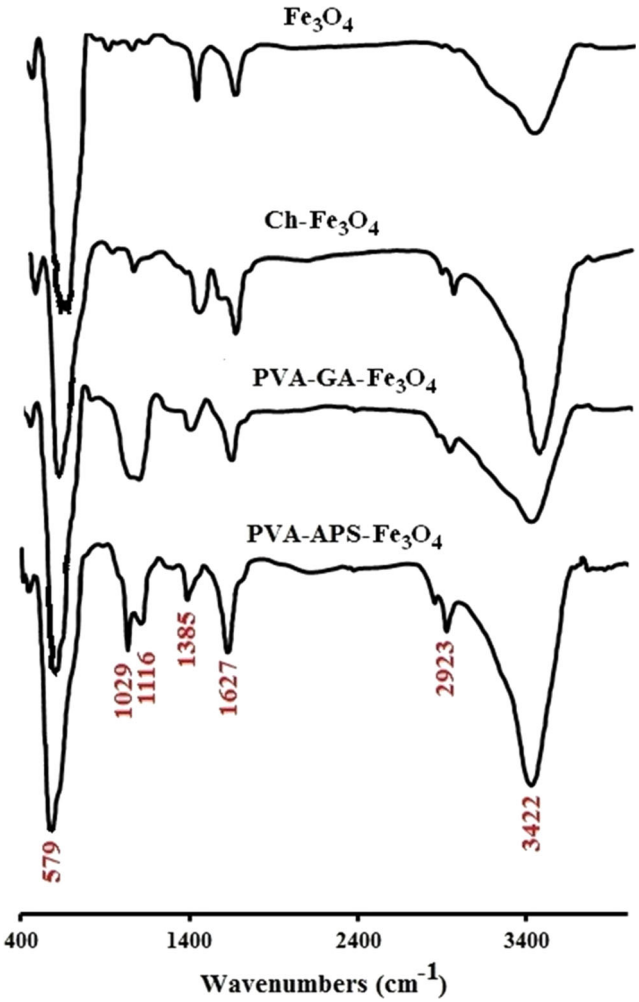

Fig. 2 FTIR spectra of samples

Scanning electron microscopy (SEM, Hitachi S-4160) and transmission electron microscopy (TEM, Philips EM208S at an accelerating voltage of 150 kV) techniques were applied to observe the morphology and size of nanoparticles. Figure 1b and d are SEM and TEM images of Fe_3O_4 nanoparticles, respectively. The obtained magnetic Fe_3O_4 nanoparticles had almost spherical or quasi-spherical shape with 4.9–27.3 nm size in diameter. The images of Ch–Fe_3O_4 nanoparticles (Fig. 1c, f) confirmed that during coating process, morphology of Fe_3O_4 nanoparticles has not changed. A chitosan layer can be seen on the surface of Fe_3O_4 nanoparticles in TEM image.

To experimentally investigate the influence of cross-linking agent type on the rate of diffusion and release of drug molecules in nanohydrogel matrix, PVA was reacted with Ch–Fe_3O_4 nanoparticles via GA and APS. Scheme 1 shows the proposed mechanism for the reaction between aldehyde functional groups in GA and OH and NH_2 functional groups in PVA and chitosan. GA usually cross-links by reacting each aldehyde with two free unprotonated amine and alcohol groups, to form Schiff's base bridges. In acidic medium, the carbon alpha to the aldehyde group turn to a highly reactive carbocation. The –OH and –NH_2 functional groups in PVA and chitosan can make a nucleophilic attack to this carbocation, and then, H^+ is reproduced in the medium. The final product of OH functional group and GA is a stabilized hemiacetal group in the low pH of system. Moreover, the reaction between amine functional group with the aldehyde forms an imine bond. GA can be polymerized to generate intermolecular cross-linking with larger distances [19–21]. On other hand, cross-linking with APS occurs via a radical mechanism (Scheme 2) [22, 23]. APS radically initiates the cross-linking of PVA and chitosan to each other.

The samples were analyzed by a FTIR Spectrum System (Magna-IR spectrophotometer 550) in the infrared region from 400 to 4000 cm^{-1}. The FTIR spectra of samples are shown in Fig. 2. The characteristic peak of Fe–O stretching band at 579 cm^{-1} could prove the presence of Fe_3O_4 nanoparticles in all samples. The broad band at 3100–3600 cm^{-1} for Fe_3O_4 and modified nanoparticles was related to the O–H vibration on the surface of these nanoparticles. The characteristic absorption bands appeared at 1029 cm^{-1} can be assigned to C–O stretching. Furthermore, the vibrational band observed at 2923 cm^{-1} corresponded to the stretching C–H of alkyl groups.

SEM and TEM images of nanohydrogels are presented in Fig. 3. The images indicated that Fe_3O_4 nanoparticles are completely encapsulated in the cross-linked chitosan and PVA matrix in non-specialized shapes.

The hydrodynamic sizes of nanohydrogels were measured by using dynamic light scattering (DLS) (Malvern-DTS Ver 4.20) at room temperature (Fig. 4). The results were depended on sonication time. After 5-min sonication, both nanohydrogels presented large hydrodynamic size, and PVA-APS and PVA-GA-Fe_3O_4 nanohydrogels had 1270 and 977 nm, respectively. After 15-min sonication, these sizes reduced to 223 and 143 nm, respectively. The hydrodynamic size can affect the clearance mechanism of drug delivery system from the blood stream. Furthermore, it will be affected the permeation of nanocarries from vascular [24]. Therefore, nanohydrogel must be completely dispersed before using in biological environment.

It has been proved that surface charge of nanoparticles is a major factor of cellular internalization. Furthermore, charge-based uptake depends on cell type. It has reported that positively charged nanoparticles have enhanced internalization in different cancer cell types, such as MCF-7 cells, HeLa cells, and endothelial cells, compared with negatively charged nanoparticles [2].

The large value of surface charge causes the more stabilization in the dispersion. However, highly charged coatings in biological fluids are instable due to plasma protein adsorption. Drug delivery systems with neutral or low negative charge surface have low plasma protein adsorption and non-specific cellular interaction. Therefore, by reducing the surface charge

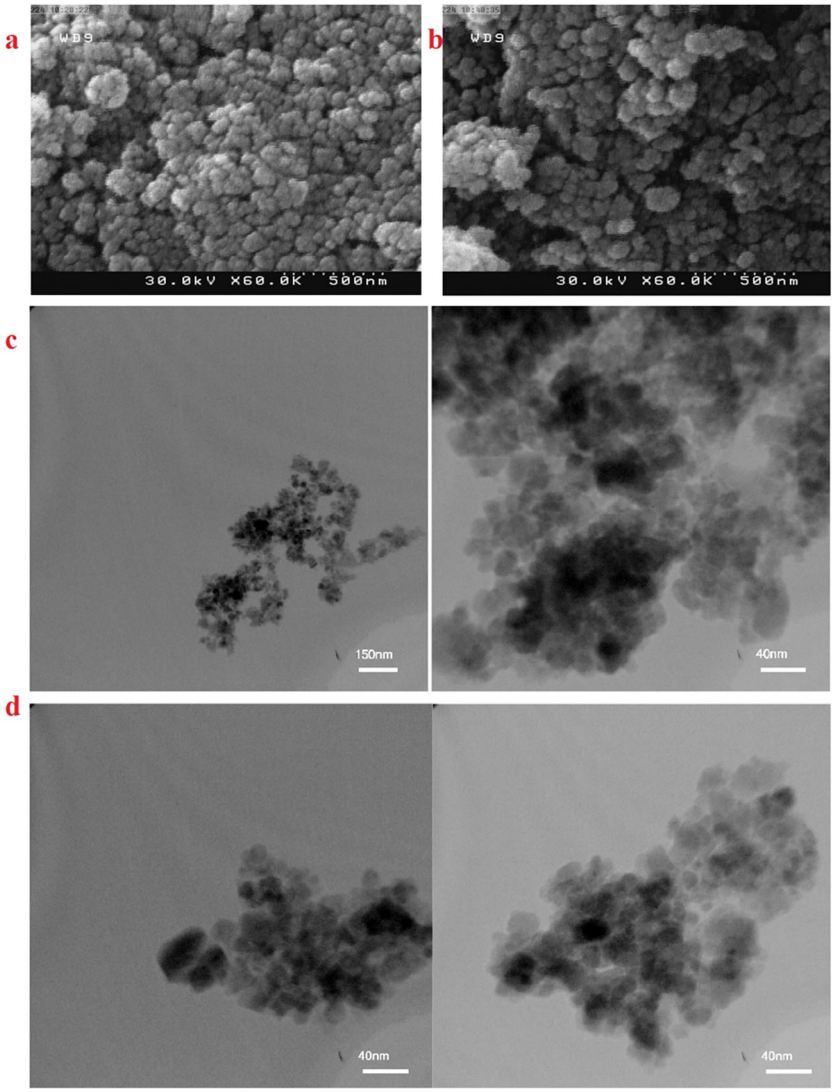

Fig. 3 **a** SEM image of PVA-APS-Fe_3O_4. **b** SEM image of PVA-GA-Fe_3O_4. **c** TEM images of PVA-APS-Fe_3O_4. **d** TEM images of PVA-GA-Fe_3O_4 nanohydrogels

and using hydrophilic matter stability of nanomaterial in the body can be improved [24, 25]. The zeta potential of nanohydrogels was measured to evaluate the surface charge. PVA-APS and PVA-GA-Fe_3O_4 nanohydrogels had zeta potential of − 6.87 and − 11.4 mV, respectively.

Total iron content was quantified by flame atomic absorption spectrometry (AAS) to evaluate the amount of non-solid coating in each nanomaterial. It is calculated from the AAS results that coating amounts are about 12.09, 44.71, and 37.34% for Ch–Fe_3O_4, PVA-APS-Fe_3O_4, and PVA-GA-Fe_3O_4, respectively (Fig. 5a).

The magnetic properties of samples were studied by using a vibrating sample magnetometer (VSM) (Meghnatis Daghigh Kavir Co, Iran) at room temperature. Magnetization hysteresis loops at 25 °C of nanomaterials are presented in Fig. 5b. All samples were superparamagnetic, and the hysteresis curves showed no hysteresis. The saturation magnetization (Ms) values for Fe_3O_4, Ch–Fe_3O_4, PVA-APS-Fe_3O_4, and PVA-GA-Fe_3O_4 were 57.8, 49.4, 31.5, and 36.4 emu g^{-1}, respectively. The reduction in Ms values is associated to the presence of non-magnetic coating in nanomaterial. These magnet can be guided to the target tissue by an external magnetic field which is referred to as magnetic targeting [26]. Superparamagnetic characteristics of these nanomaterial causes that they have no magnetic interaction in the absence of magnetic field [27]. This property is important for the nanomaterial to be used for biological application as an MRI contrast agent which prevents nanoparticles from magnetic aggregation. Therefore, they can redisperse rapidly when the magnetic field is removed [17]. Superparamagnetic iron oxide nanoparticles could be used in magnetic hyperthermia, an alternating magnetic field. In this field, superparamagnetic nanomaterials generate heat that provides intended therapeutic effect [6].

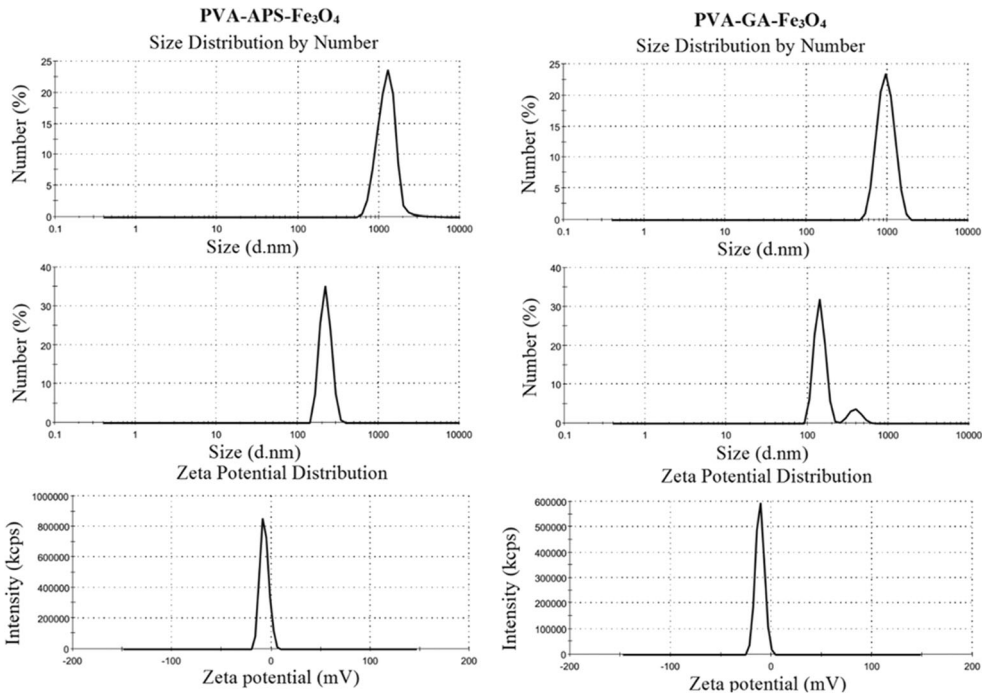

Fig. 4 Size and zeta potential of nanohydrogels

Adsorption of plasma proteins onto the surface of circulating nanomaterial in blood (opsonization) can affect or prevent their functions. This process depends on various factors such as size, surface charge, hydrophobicity, and surface chemistry. Specifically, hydrophobic and highly charged nanomaterial have short circulation because of adsorption of opsonization which can lead to identification by the reticuloendothelial system (RES), followed by eliminating from circulation [2, 5].

Protein interaction of samples was evaluated by the UV-Vis spectroscopy method (Fig. 6). BSA and IgG were chosen as protein models. Albumin and IgG are the most abundant plasma protein in human blood [28]. BSA was chosen as a model protein because it is similar to human serum albumin (HSA) in 76% [29]. Moreover, the selected proteins have different isoelectronic points. IgG has isoelectric point more than 5.5 and interacts with negatively charged surfaces. On the other hand, albumin has isoelectric point less than 5.5 and interacts with positively charged surfaces [30].

As have been shown in Fig. 6, in BSA solution, both PVA-APS and PVA-GA-Fe_3O_4 with negative surface charge have the least adsorption of albumin. But, other nanoparticles showed higher albumin adsorption. In IgG solution, the result is completely different and Ch–Fe_3O_4 nanoparticles have shown the lowest adsorption of IgG because of their highly positive surface charge.

Incorporation of ascorbic acid as a model of hydrophilic drug into nanohydrogels was achieved via diffusion of drug molecules within nanohydrogel matrix. Encapsulation within a nanocarrier protects the drug from protein binding and inactivation. Furthermore, the majority of drug remains within the nanocarrier during circulation. Therefore, potential toxicity in non-target site will be minimized [3].

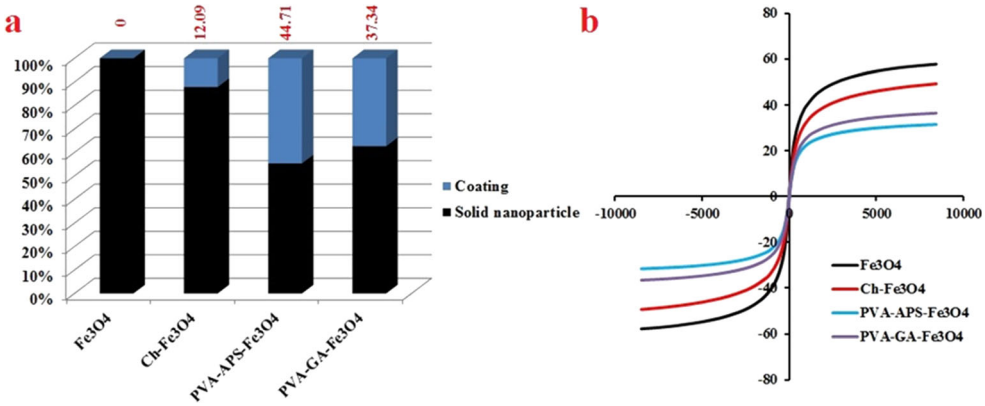

Fig. 5 **a** Solid and coating content obtained by AAS. **b** Magnetization hysteresis loops of samples

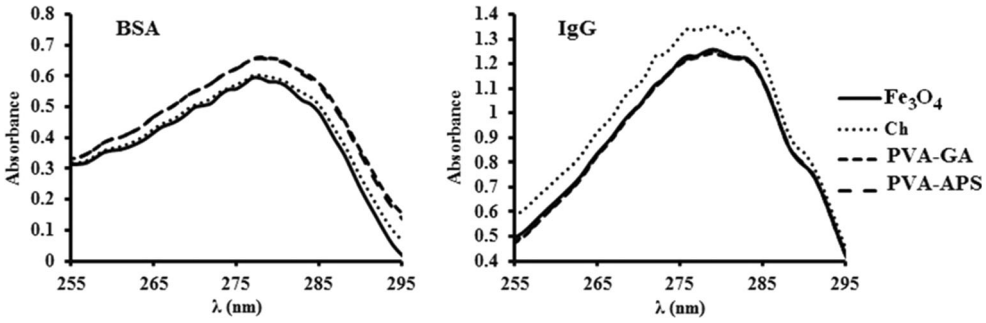

Fig. 6 UV spectra of protein solution after separation from samples

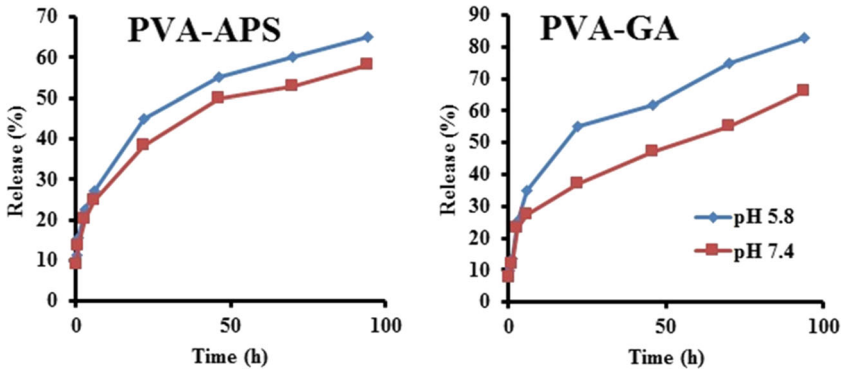

Fig. 7 Drug release profiles from nanohydrogels

The loading capacity and release behavior of nanohydrogel was evaluated by the UV-Vis spectrophotometry method at 254 nm. The drug loading contents and drug entrapment efficiency were 5.9% and 12.4% for PVA-APS-Fe_3O_4 and 10% and 10.38% for PVA-GA-Fe_3O_4 nanohydrogels, respectively.

Controlled release is related to use of polymeric materials to release incorporated drugs at a controlled manner and rate for a desired period of time [7]. Drug molecules can be released from nanocarries via diffusion through water-filled pores. Furthermore, erosion of polymer matrix can be another factor for release of drug molecules. The process of diffusion is related to the random movement of drug molecules because of a concentration gradient. Polymeric matrix of nanohydrogels can immediately absorb water. This leads to occupy pores with water, and the size of pores becomes larger. Thus, the release could be facilitated [6]. The release profiles of nanohydrogel are shown in Fig. 7. The initial fast release of drug could be related to drug molecules that are trapped near the surface [31]. The release profile showed that both nanohydrogels had more and faster release in acidic medium. But PVA-GA-Fe_3O_4 nanohydrogels were more pH-sensitive. They were faster and had more ascorbic acid compared with the PVA-APS-Fe_3O_4 nanohydrogels.

Both drug loading content and drug release behavior showed that they have been affected by cross-linking agent (Scheme 3). APS cross-links polymers via a radical mechanism. Therefore, polymer are connected with each other tightly. This prevents nanohydrogel to become more swollen in aqueous medium. On the other hand, GA makes a bridge between polymers and is able to change its conformation. Thus, more swelling can occur, especially in acidic environment.

Today, responsive drug delivery systems have become a trend in drug delivery technology. These systems can enhance

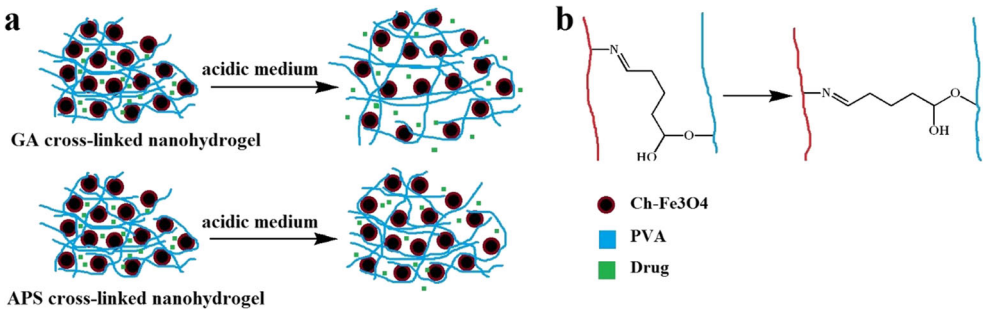

Scheme 3 **a** Swelling process affected by cross-linking agent. **b** Changing of conformation for GA

bioavailability and limit the side effects of drug. In various sensitive drug release systems, pH-responsive system has received a lot of attention. Compared with the healthy blood and normal tissue, the pH is low for most diseased tissues such as inflammation, infection, and malignancy tissue, and even lower for the cell organelles. Therefore, the design of pH-sensitive drug delivery systems, which have a slow drug release in normal tissue medium and a fast drug release in the acidic diseased tissue medium, can make a variety of therapy target and reduce side effects of drug [32].

4 Conclusion

The present study described a successful preparation of nanohydrogels of PVA, chitosan, and Fe_3O_4 nanoparticles. First, magnetite nanoparticles were synthesized in alkaline medium by sonication. Then, these nanoparticles were coated with chitosan. To obtain nanohydrogels, PVA cross-linked with Ch–Fe_3O_4 nanoparticles in the presence of GA or APS. The samples were characterized by various method including the XRD, FT-IR, AAS, zeta potential, XRD, SEM, TEM, and VSM. All samples had superparamagnetic property that prevents from magnetic agglomeration in biological environment in the absence of external magnetic field. We used BSA and IgG as models of plasma proteins to examine the protein adsorption of samples by the UV spectroscopy method. Nanohydrogels had lowest adsorption in BSA solution. Drug release behavior showed that nanohydrogels crosslinked with GA had more pH-sensitivity. GA makes a bridge between polymers and allows them to be more swollen in acidic environment. But, APS connects polymers tightly and less swelling will occur.

Compliance with Ethical Standards

Conflict of Interest The authors declare that they have no conflict of interest.

Research Involving Humans and Animals Statement None.

Informed Consent None.

Funding Information There are no sources of financial funding and support.

References

1. Fu, Y., & Kao, W. J. (2010). Drug release kinetics and transport mechanisms of non-degradable and degradable polymeric delivery systems. *Expert Opinion on Drug Delivery, 7*(4), 429–444.
2. Blanco, E., Shen, H., & Ferrari, M. (2015). Principles of nanoparticle design for overcoming biological barriers to drug delivery. *Nature Biotechnology, 33*, 941.
3. Kai, M. P., et al. (2015). Evaluation of drug loading, pharmacokinetic behavior, and toxicity of a cisplatin-containing hydrogel nanoparticle. *Journal of Controlled Release, 204*, 70–77.
4. Vall, M., et al. (2017). Effects of amine modification of mesoporous magnesium carbonate on controlled drug release. *International Journal of Pharmaceutics, 524*(1), 141–147.
5. Veiseh, O., Gunn, J. W., & Zhang, M. (2010). Design and fabrication of magnetic nanoparticles for targeted drug delivery and imaging. *Advanced Drug Delivery Reviews, 62*(3), 284–304.
6. Kamaly, N., et al. (2016). Degradable controlled-release polymers and polymeric nanoparticles: Mechanisms of controlling drug release. *Chemical Reviews, 116*(4), 2602–2663.
7. Alexis, F. (2005). Factors affecting the degradation and drug-release mechanism of poly(lactic acid) and poly[(lactic acid)-co-(glycolic acid)]. *Polymer International, 54*(1), 36–46.
8. Bowers, D. T., Botchwey, E. A., & Brayman, K. L. (2015). Advances in local drug release and scaffolding design to enhance cell Therapy for diabetes. *Tissue Engineering Part B: Reviews, 21*(6), 491–503.
9. Craciun, A. M., et al. (2019). Nitrosalicyl-imine-chitosan hydrogels based drug delivery systems for long term sustained release in local therapy. *Journal of Colloid and Interface Science, 536*, 196–207.
10. Rutkowski, S., et al. (2019). Magnetically-propelled hydrogel particle motors produced by ultrasound assisted hydrodynamic electrospray ionization jetting. *Colloids and Surfaces B: Biointerfaces, 175*, 44–55.
11. Prabaharan, M. (2015). Chitosan-based nanoparticles for tumor-targeted drug delivery. *International Journal of Biological Macromolecules, 72*, 1313–1322.
12. Shu, X. Z., & Zhu, K. J. (2002). Controlled drug release properties of ionically cross-linked chitosan beads: the influence of anion structure. *International Journal of Pharmaceutics, 233*(1), 217–225.
13. Kamoun, E. A., et al. (2015). Crosslinked poly(vinyl alcohol) hydrogels for wound dressing applications: A review of remarkably blended polymers. *Arabian Journal of Chemistry, 8*(1), 1–14.
14. Zhang, D., et al. (2015). Carboxyl-modified poly(vinyl alcohol)-crosslinked chitosan hydrogel films for potential wound dressing. *Carbohydrate Polymers, 125*, 189–199.
15. Rutkowski, S., et al. (2019). Magnetically-guided hydrogel capsule motors produced via ultrasound assisted hydrodynamic electrospray ionization jetting. *Journal of Colloid and Interface Science, 541*, 407–417.
16. Hu, N., et al. (2017). Forecastable and guidable bubble-propelled microplate motors for cell transport. *Macromolecular Rapid Communications, 38*(11), 1600795.
17. Shagholani, H., Ghoreishi, S. M., & Mousazadeh, M. (2015). Improvement of interaction between PVA and chitosan via magnetite nanoparticles for drug delivery application. *International Journal of Biological Macromolecules, 78*, 130–136.
18. Kayal, S., & Ramanujan, R. V. (2010). Doxorubicin loaded PVA coated iron oxide nanoparticles for targeted drug delivery. *Materials Science and Engineering: C, 30*(3), 484–490.
19. Guyomard-Lack, A., et al. (2015). Ion segregation in an ionic liquid confined within chitosan based chemical ionogels. *Physical Chemistry Chemical Physics, 17*(37), 23947–23951.
20. Farris, S., et al. (2009). Development of polyion-complex hydrogels as an alternative approach for the production of bio-based polymers for food packaging applications: a review. *Trends in Food Science & Technology, 20*(8), 316–332.
21. Gonçalves, V. L., et al. (2005). Effect of crosslinking agents on chitosan microspheres in controlled release of diclofenac sodium %J. *Polímeros., 15*, 6–12.
22. Kumar, P., et al. (2012). Novel high-viscosity polyacrylamidated chitosan for neural tissue engineering: Fabrication of anisotropic neurodurable caffold via molecular disposition of persulfate-

mediated polymer slicing and complexation. *International Journal of Molecular Sciences, 13*(11), 13966.
23. Li, J., et al. (2015). Cross-linking of poly(vinyl alcohol) with N,N′-methylene bisacrylamide via a radical reaction to prepare pervaporation membranes. *RSC Advances, 5*(26), 19859–19864.
24. Shagholani, H., & Ghoreishi, S. M. (2017). Investigation of tannic acid cross-linked onto magnetite nanoparticles for applying in drug delivery systems. *Journal of Drug Delivery Science and Technology, 39*, 88–94.
25. Khoee, S., Shagholani, H., & Abedini, N. (2015). Synthesis of quasi-spherical and square shaped oligoamino-ester graft-from magnetite nanoparticles: Effect of morphology and chemical structure on protein interactions. *Polymer, 56*, 207–217.
26. Lee, N., et al. (2015). Iron oxide based nanoparticles for multimodal imaging and magnetoresponsive therapy. *Chemical Reviews, 115*(19), 10637–10689.
27. Laurent, S., et al. (2014). Superparamagnetic iron oxide nanoparticles for delivery of therapeutic agents: opportunities and challenges. *Expert Opinion on Drug Delivery, 11*(9), 1449–1470.
28. Kratz, F., & Elsadek, B. (2012). Clinical impact of serum proteins on drug delivery. *Journal of Controlled Release, 161*(2), 429–445.
29. Li, X., et al. (2012). Interaction of bovine serum albumin with self-assembled nanoparticles of 6-O-cholesterol modified chitosan. *Colloids and Surfaces B: Biointerfaces, 92*, 136–141.
30. Boyer, C., et al. (2010). The design and utility of polymer-stabilized iron-oxide nanoparticles for nanomedicine applications. *Npg Asia Materials, 2*, 23.
31. Wu, Y., et al. (2006). Preparation and characterization of chitosan–poly(acrylic acid) polymer magnetic microspheres. *Polymer, 47*(15), 5287–5294.
32. Zou, X., et al. (2015). Preparation and drug release behavior of pH-responsive bovine serum albumin-loaded chitosan microspheres. *Journal of Industrial and Engineering Chemistry, 21*, 1389–1397.